Tetrahedron Letters 50 (2009) 802–806

Contents lists available at ScienceDirect

Tetrahedron Letters

journal homepage: www.elsevier.com/locate/tetlet

Novel sesquiterpenes and norergosterol from the soft corals *Nephthea erecta* and *Nephthea chabroli*

Shi-Yie Cheng [a], Ya-Chiang Huang [a], Zhi-Hong Wen [a], Shu-Fen Chiou [a], Shang-Kewi Wang [b], Chi-Hsin Hsu [a], Chang-Feng Dai [c], Chang-Yih Duh [a,d,*]

[a] *Department of Marine Biotechnology and Resources, National Sun Yat-Sen University, Kaohsiung 804, Taiwan*
[b] *Department of Microbiology, Kaohsiung Medical University, Kaohsiung 807, Taiwan*
[c] *Institute of Oceanography, National Taiwan University, Taipei, Taiwan*
[d] *Center of Asia-Pacific Marine Researches, National Sun Yat-sen University, Kaohsiung, Taiwan*

A R T I C L E I N F O

Article history:
Received 1 November 2008
Revised 27 November 2008
Accepted 1 December 2008
Available online 6 December 2008

Keywords:
Nephthea erecta
Calamenene-type
Mercaptan
sec-Germacrane
Norergosterol
Nephthea chabroli
Anti-inflammatory activity
Antimicrobial activities

A B S T R A C T

Chemical investigations on the acetone extract of the Formosan soft coral *Nephthea erecta* have afforded a new calamenene-type sesquiterpene with a mercaptan group at C-15, erectathiol (**1**), and a previously reported sesquiterpenoid, (+)-*trans*-calamenene (**2**). A novel *sec*-germacrane sesquiterpene (**3**), along with a novel norergosterol, chabrosterol (**4**), possessing a 19-norergostane skeleton, was isolated from the other soft coral *Nephthea chabroli*. The structures of these metabolites were elucidated through extensive spectroscopic analyses. In vitro anti-inflammatory activity of **1** and **4** (10 μM) significantly reduced the levels of the iNOS protein (58.0 ± 6.5% and 12.4 ± 2.9%) and COX-2 protein (108.7 ± 4.5% and 45.2 ± 5.4%). In addition, metabolite **1** (166 μg/disk) exhibited antimicrobial activities against a small panel of bacterial strains.

© 2008 Elsevier Ltd. All rights reserved.

The family Nephtheidae has been proved to be a rich source of bioactive sesquiterpenoids and steroids.[1–10] Recently, many savants have paid much attention to these secondary metabolites due to their biological activities. A number of sesquiterpenoids have shown an array of biological activities such as insecticidal[2] and cytotoxic activities.[3,4] Some of steroids were reported to possess cytotoxic[5–8] and anti-inflammatory activities.[9] In the course of our ongoing endeavor to discover bioactive secondary metabolites from marine organisms, chemical investigations of the Formosan soft corals *Nephthea erecta* Kükenthal and *Nephthea chabroli* Audouin were undertaken.[4,6,7]

Chromatographic separation on the acetone extract of the soft coral *N. erecta* led to the isolation of a new calamenene-type sesquiterpene, erectathiol (**1**), together with a known calamenene-type sesquiterpene, (+)-*trans*-calamenene (**2**) (Fig. 1), which was also isolated from the soft coral *Sarcophyton glaucum*[11a] and the liverwort *Conocephalum conicum*.[11b] We have obtained a novel *sec*-germacrane sesquiterpene, (2*E*,6*E*)-3-isopropyl-6-methyl-10-oxoundeca-2,6-dienal (**3**), and a novel 19-norergosterol, chabrosterol (**4**) (Fig. 1), from the other soft coral *N. chabroli*. To the best of our knowledge, erectathiol (**1**) (possessing a rare mercaptan moiety at C-15), (2*E*,6*E*)-3-isopropyl-6-methyl-10-oxoundeca-2,6-dienal (**3**) (a novel *sec*-germacrane skeleton), and chabrosterol (**4**) (a novel 19-norergostane skeleton) are reported from marine soft corals for the first time. The details of isolation and structural elucidation of these isolated metabolites are discussed in this Letter. The in vitro anti-inflammatory activities of **1** and **4** were measured, and the antibacterial activities against *Enterobacter aerogenes* (ATCC13048), *Serratia marcescens* (ATCC25419), *Salmonella enteritidis* (ATCC13076), *Yersinia enterocolitica* (ATCC23715), and *Shigella sonnei* (ATCC11060) of **1** were also evaluated in vitro. Meanwhile, the plausible biosynthetic pathways for formation of these isolated metabolites were postulated, see below.

The soft corals *N. erecta* and *N. chabroli* were collected by hand using scuba at the Green Island and Siaoliouciou Island off Taiwan, respectively. Both specimens were identified by Prof. C.-F. Dai, and voucher specimens were deposited in the Department of Marine Biotechnology and Resources, National Sun Yat-sen University.

The acetone extract of *N. erecta* was concentrated to a brown gum, which was partitioned with EtOAc and H_2O. The EtOAc-soluble residue (35.0 g) was subjected to CC on silica gel using *n*-hexane–EtOAc mixtures of increasing polarity for elution, to fractionate 40 fractions. Fraction 2 (6.0 g) was subjected to CC on

* Corresponding author. Tel.: +886 7 5252000x5036; fax: +886 7 5255020.
E-mail address: yihduh@mail.nsysu.edu.tw (C.-Y. Duh).

0040-4039/$ - see front matter © 2008 Elsevier Ltd. All rights reserved.
doi:10.1016/j.tetlet.2008.12.002

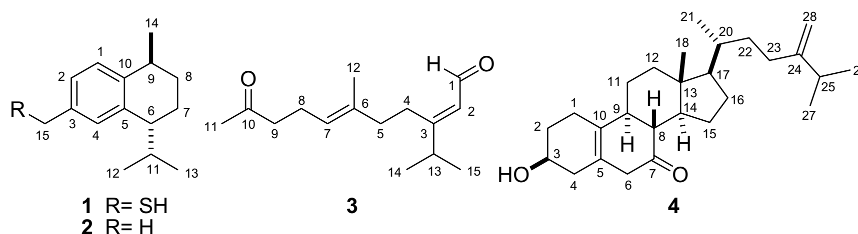

Figure 1. Structures of metabolites **1–4**.

silica gel to obtain **2** (1.0 mg). Similarly, metabolite **1** (4.0 mg) was purified by NP-HPLC using *n*-hexane–CH_2Cl_2 (90:1). In the same manner, the EtOAc fraction (100.0 g) of the other soft coral *N. chabroli* was subjected to CC on silica gel to furnish 40 fractions. Duplicate samples (2.0 g) of fraction 10 (7.5 g) was fractionated over a PR-18 gel column using MeOH–H_2O mixtures of increasing polarity for elution, to separate six subfractions. Subfraction 2 (26 mg) was subjected to a PR-18 gel column to obtain a mixture (12 mg) that was further purified by RP-HPLC using 75% MeOH in H_2O to yield **3** (2 mg). Fraction 12 (4.0 g) was fractionated over Sephadex LH-20 (100% acetone) to produce 40 subfractions. Subfraction 36 (102 mg) was subjected to CC on silica gel to obtain a mixture (64 mg) that was further purified by RP-HPLC using 95% MeOH in H_2O to give **4** (2 mg).

Erectathiol (**1**)[12] was obtained as a light yellow oil. The molecular formula was determined to be $C_{15}H_{22}S$, as deduced from HRFABMS (*m/z* 235.1521, $[M+H]^+$) and ^{13}C NMR spectroscopic data (Table 1), implying the existence of five degrees of unsaturation. The NMR spectrum (Table 1) showed a trisubstituted phenyl moiety [^1H NMR δ_H 7.16, 7.01 (*d*, J = 8.0 Hz, 1H each), and 7.07 (br s, 1H); ^{13}C NMR δ_C 127.0, 126.1, 135.7, 128.7, 140.2, and 142.1]. The above functionalities also account for four of the five degrees of unsaturation, suggesting a bicyclic structure in **1**. Moreover, the ^{13}C NMR and DEPT spectra revealed 15 carbon signals, including three methyls, three methylenes, six methines, and three quaternary carbons. The above data of **1** were similar to those of (−)-*trans*-calamenene,[11b] except for the replacement of the methyl by a mercaptan group [δ_H 3.89, 3.81 (d, J = 10.8 Hz, 1H each) and δ_C 32.9 (t)] at C-15.[13] This was supported by HMBC spectrum that long-range ^1H–^{13}C correlations were observed from H-15 to C-2, C-3, and C-4. Thus, the planar structure of **1** was established unambiguously.

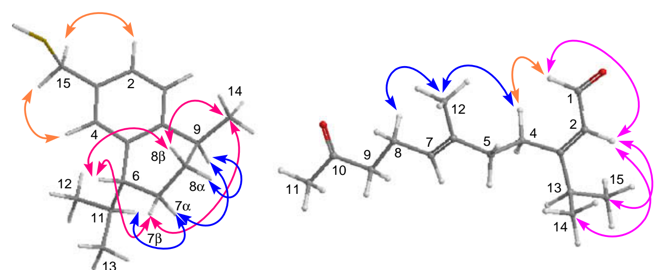

Figure 2. Key NOE correlations and computer-generated perspective model using MM2 force field calculations for **1** and **3**.

The NOE correlations (Fig. 2) between H-7β with the following protons of H-6 and Me-14, and Me-14 and H-8β suggested that these protons were oriented on the same side of the cyclohexene moiety, while the isopropyl group at C-6 was oriented on the opposite side. Moreover, the absolute stereochemistry of **1** was further elucidated by comparison of its optical rotation, $[\alpha]_D^{24}$ +23 (*c* 0.4, $CHCl_3$), with that of (−)-*trans*-calamenene.[11b] From the above-mentioned findings, metabolite **1** was formulated as [(6*R*,9*S*)-6-isopropyl-9-methyl-6,7,8,9-tetrahydronaphthalen-3-yl]methanethiol.

Metabolite **3**[14] analyzed for a molecular formula of $C_{15}H_{24}O_2$, according to the interpretation of its HRESIMS and NMR spectroscopic data (Table 1), implies four degrees of unsaturation. The IR absorptions of **3** at 2874 and 1671 cm^{-1} revealed the presence of a conjugated aldehyde functionality. This was further indicated from the ^1H NMR signals at δ 9.93 (1H, d, J = 8.0 Hz) and 5.78 (1H, d, J = 8.0 Hz), and ^{13}C NMR signals at δ 189.5 (CH, C-1), 124.1 (CH, C-2), and 170.2 (qC, C-3). The UV absorption maxima

Table 1
^1H and ^{13}C NMR spectroscopic data of metabolites **1** and **3**[a]

C/H	1				3			
	^{13}C	^1H	COSY	HMBC	^{13}C	^1H	COSY	HMBC
1	127.0 (d)[b]	7.16 d (8.0)[c]	2	3, 5	189.5 (d)[b]	9.93 d (8.0)[c]	2	2
2	126.1 (d)	7.01 d (8.0)	1	4, 10	124.1 (d)	5.78 d (8.0)	1	4, 13
3	135.7 (s)				170.2 (s)			
4	128.7 (d)	7.07 s		2, 10	30.5 (t)	2.63 t (8.0)	5	2, 3, 5, 6, 13
5	140.2 (s)				41.0 (t)	2.17 t (8.0)	4	6, 7
6	43.8 (d)	2.71 m	7, 11		133.6 (s)			
7	21.4 (t)	α: 1.61 m; β: 1.83 m	6, 8		123.6 (d)	5.11 t (6.4)	8	5, 8
8	30.6 (t)	α: 1.95 m; β: 1.36 m	7, 9		23.3 (t)	2.26 dd (7.6, 6.4)	7, 9	6, 7, 10
9	32.7 (d)	2.75 m	8, 14		44.0 (t)	2.46 t (7.6)	8	7, 10
10	142.1 (s)				206.1 (s)			
11	31.9 (d)	2.23 m	6, 12, 13		30.8 (q)	2.14 s		9, 10
12	17.4 (q)	0.71 d (6.8)	11	6, 11,13	17.2 (q)	1.66 br s		5, 6, 7
13	21.3 (q)	1.01 d (6.8)	11	6, 11,13	36.5 (d)	2.41 septet (6.8)		3
14	22.3 (q)	1.26 d (6.8)	9	8, 9, 10	22.4 (q)	1.11 d (6.8)		3, 13, 15
15	32.9 (t)	α: 3.89 d (10.8)						
		β: 3.81 d (10.8)		2, 3, 4	22.4 (q)	1.11 d (6.8)		3, 13, 14

[a] Spectra were measured in $CDCl_3$ (^1H, 400 MHz and ^{13}C, 100 MHz).
[b] Multiplicities are deduced by HSQC and DEPT experiments.
[c] J values (in Hz) are in parentheses.

Table 2
^{1}H and ^{13}C NMR spectroscopic data of chabrosterol (**4**)[a]

C/H	4			
	^{13}C	^{1}H	COSY	HMBC
1	24.4 (t)[b]	α: 2.15 m; β: 2.59 m	2	
2	28.8 (t)	α: 1.69 m; β: 1.80 m	1, 3	
3	65.0 (d)	4.13 m	2, 4	
4	31.3 (t)	α: 2.52 m; β: 2.27 m	3	5
5	158.6 (s)			
6	43.2 (t)	α: 2.01 d (16.5)[c]; β: 2.49 dd (16.5, 3.5)		5, 7, 8, 10
7	199.1 (s)			
8	39.4 (d)	1.82 m	9, 14	
9	46.2 (d)	2.00 m	8, 11	5, 7, 8
10	128.8 (s)			
11	24.5 (t)	α: 1.95 m; β: 1.43 m	9, 12	
12	39.8 (t)	α: 1.29 m; β: 2.09 m	11	
13	42.5 (s)			
14	55.0 (d)	1.29 m	8, 15	
15	23.4 (t)	α: 1.58 m; β: 1.09 m	14, 16	
16	28.1 (t)	α: 1.89 m; β: 1.29 m	15, 17	
17	55.9 (d)	1.19 m	16, 20	
18	12.0 (q)	0.71 s		12, 13, 14, 17
20	35.6 (d)	1.43 m	17, 21, 22	
21	18.6 (q)	0.96 d (6.5)	20	17, 20, 22
22	34.6 (t)	α: 1.16 m; b: 1.53 m	20, 23	
23	30.9 (t)	α: 1.88 m; b: 2.09 m	22	24
24	156.7 (s)			
25	33.8 (d)	2.23 septet (6.5)	26, 27	
26	21.8 (q)	1.03 d (6.5)	25	24, 25, 27
27	22.0 (q)	1.03 d (6.5)	25	24, 25, 26
28	106.0 (t)	α: 4.66 s; b: 4.72 s		23, 25

[a] Spectra were measured in $CDCl_3$ (^{1}H, 500 MHz and ^{13}C, 125 MHz).
[b] Multiplicities are deduced by HSQC and DEPT experiments.
[c] *J* values (in Hz) are in parentheses.

241 nm suggested the aforementioned chromophore. A keto-carbonyl group was recognized as being present in **3** from its ^{13}C NMR signal at δ 206.1 (qC, C-10), as well as from a broad IR absorption at 1716 cm^{-1}. Moreover, the ^{1}H and ^{13}C NMR spectroscopic data of **3** contained resonances for a trisubstituted double bond at C-6 and C-7 [δ_H 5.11 (t, J = 6.4 Hz, 1H); δ_C 133.6 (qC) and 123.6 (CH)]. The above functionalities accounted for four of the four degrees of unsaturation, suggesting a linear structure for **3**.

By interpretation of ^{1}H–^{1}H COSY correlations, it was possible to establish four partial structures of consecutive proton systems extending from H-1 to H-2, from H_2-4 to H_2-5, from H_3-14 to H_3-15 through H-13, and from H_2-9 to H_3-12 through H-7 and H_2-8, as well as long-range COSY correlation between H_3-12 and H-7. Moreover, the connectivities of these partial structures were further established by the HMBC correlations. On the basis of the above observations, the *sec*-germacrane structure of **3** was established unambiguously. The geometry of the trisubstituted olefins was assigned as *E* based on the γ-effect of the olefinic methyl signal for C-12 (less than 20 ppm) and the NOESY correlation between H_2-8 and H_3-12. The NOE correlations (Fig. 2) between H-1/H_2-4, H-2/H_3-14, and H-2/H_3-15 indicated the *s*-trans geometry of the conjugated aldehyde moiety. All the NMR spectroscopic data of metabolite **3**, assigned by COSY, HMQC, HMBC, and NOESY correlations, were satisfactorily consistent with the structure shown as (2*E*,6*E*)-3-isopropyl-6-methyl-10-oxoundeca-2,6-dienal.

Chabrosterol (**4**)[15] was isolated as a white amorphous powder. HRESIMS of **4** exhibited a pseudo molecular ion peak at *m*/*z* 421.3085 $[M+Na]^+$ (calcd for 421.3082) and established a molecular formula of $C_{27}H_{42}O_2$, indicating seven degrees of unsaturation. The ^{13}C NMR displayed 27 carbon signals, which were identified by the assistance of the DEPT spectrum as four methyls, eleven methylenes, seven methines, and five quaternary carbons. The ^{1}H NMR signal [δ_H 4.13 (m, 1H)] (Table 2) and IR absorption at 3309 cm^{-1}, together with the observation of one oxygen-bearing carbon resonance (δ_C 65.0) in ^{13}C NMR spectrum (Table 2), revealed the presence of one hydroxyl. Furthermore, one tetrasubstituted double bond (δ_C 128.8 and 158.6), one terminal double bond (δ_C 106.0 and 156.7), and one carbonyl carbon (δ_C 199.1) were assigned from ^{13}C NMR and DEPT spectra of **4**. The above functionalities accounted for three of the seven degrees of unsaturation, suggesting a tetracyclic skeleton for **4**.

Interpretation of the ^{1}H–^{1}H COSY spectrum led to three partial structures. The connectivities of these partial structures were further established by the HMBC correlations. Moreover, the long-range ^{1}H–^{13}C correlations observed from H_2-6 to C-7, and H-9 to C-7 indicated the position of the carbonyl group at C-7. The COSY correlations from H_2-1 to H-3 through H_2-2 led the assignment of the one secondary hydroxyl group at C-3. The location of the tetrasubstituted double bond at C-5/C-10 was clarified by analysis of the HMBC correlations from H_2-4 to C-5, and H_2-6 to C-10, and H-9 to C-5. The NOESY correlations (Fig. 3) observed between H-3 and H-2α and H-4α indicated the β-oriented of the hydroxyl group at C-3. Moreover, the NOESY correlations observed between H-2β and H-1β, H-4α and H-6α, H-6β and H-8, H-9 and H-14, H-11β and H-12β, H-12β and Me-18, Me-18 and H-20, and Me-21 and

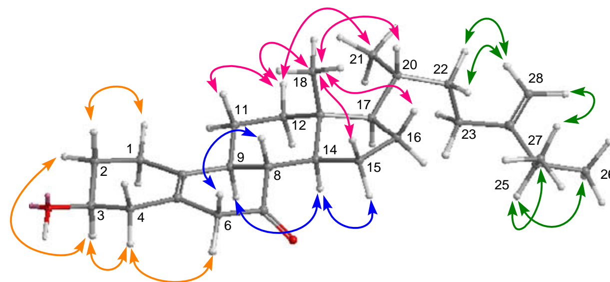

Figure 3. Key NOE correlations and computer-generated perspective model using MM2 force field calculations for **4**.

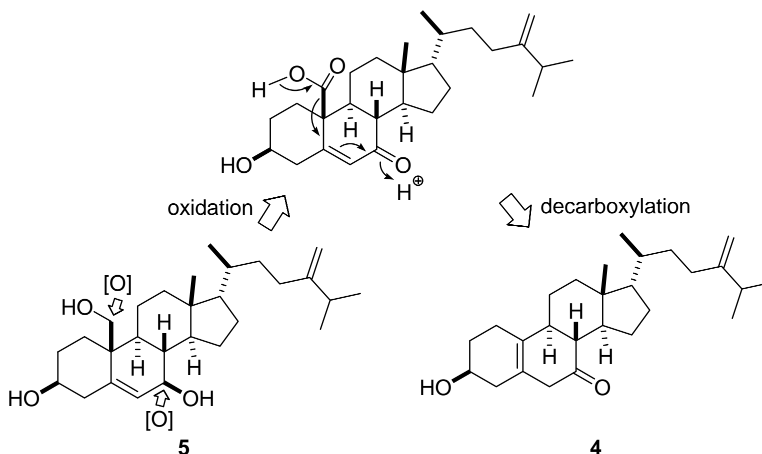

Scheme 1. Plausible biosynthetic pathway for formation of **4**.

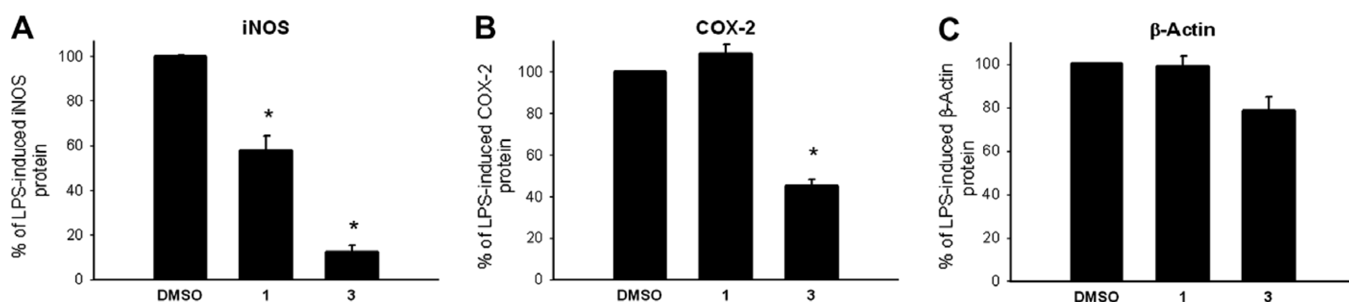

Figure 4. Effect of compounds **1** and **4** at 10 μM on the LPS-induced pro-inflammatory iNOS and on COX-2 protein expression of RAW 264.7 macrophage cells by immunoblot analysis. (A) Immunoblot of iNOS; (B) immunoblot of COX-2; (C) immunoblot of β-actin. The values are mean ± SEM. ($n = 5$). The relative intensity of the LPS alone stimulated group was taken as 100%. *Significantly different from LPS-stimulated (control) group ($^{*}P < 0.05$).

H-12β in **4** confirmed the relative configurations for each ring junction and chiral center. Thus, the structure of **4** was established unambiguously.

The main novelty of **1** is the presence of a calamanene skeleton with a rare mercaptan moiety at C-15. Erectathiol (**1**), possessing a rare mercaptan moiety, differs from previously calamenene-type sesquiterpenoids isolated from marine soft corals. Biosynthetically, it is suggested that a new approach for exhaustive transformation of **1,** in two steps mainly involves benzylic oxidation and acid-induced mercaptanization at C-15 of **1**. In addition, a plausible oxidation mechanism (dihydroxylation and oxidative cleavage of diols) of formation of metabolite **3** was postulated. It is worthwhile to mention that metabolite **4** represents the first 19-norergosterol. Because of biogenic considerations, metabolite **4** may be involved in the biosynthesis of **5**[16] through oxidation and 19-decarboxylation of **4** as depicted in Scheme 1.

Preliminary antibacterial activity revealed that metabolite **1**, at a concentration of 166 μg/disk, exhibited moderate activities against four bacterial strains, comprising *E. aerogenes*, *S. marcescens*, *Y. enterocolitica*, and *S. sonnei*. Under the same concentration, metabolite **1** revealed greater antibacterial potential than the positive control (ampicillin) against *S. enteritidis*. The antibacterial assays were carried out according to the procedure described previously.[17]

In vitro anti-inflammatory activity of metabolites **1** and **4** were tested using LPS-stimulated cells. Stimulation of RAW 264.7 cells with LPS resulted in up-regulation of the pro-inflammatory iNOS and COX-2 proteins. At a concentration of 10 μM, metabolites **1** and **4** significantly reduced the levels of the iNOS protein (58.0 ± 6.5% and 12.4 ± 2.9%) and COX-2 protein (108.7 ± 4.5% and 45.2 ± 5.4%) compared with the control cells (LPS alone) (Fig. 4). The primary anti-inflammatory results of **1** exhibited the observed activity against iNOS protein expression, but no discernible activity against COX-2 protein expression. Besides, chabrosterol **(4)**, possessing a novel 19-norergostane skeleton, showed significantly anti-inflammatory activity against LPS-stimulated RAW 264.7 cells. The anti-inflammatory assay was carried out according to the procedure described previously.[17]

Acknowledgments

Financial support was provided by the National Science Council (NSC96-2320-B-110-003-MY3) and Ministry of Education (96C031703) of the Republic of China awarded to C.-Y.D.

References and notes

1. Blunt, J. W.; Copp, B. R.; Hu, W.-P.; Munro, M. H. G.; Northcote, P. T.; Prinsep, M. R. *Nat. Prod. Rep.* **2008**, *25*, 35–94. and literature cited in previous review.
2. Handayani, D.; Edrada, R. A.; Proksch, P.; Wray, V.; Witte, L. *J. Nat. Prod.* **1997**, *60*, 716–718.
3. Duh, C.-Y.; Wang, S.-K.; Weng, Y.-L.; Chiang, M. Y.; Dai, C.-F. *J. Nat. Prod.* **1999**, *62*, 1518–1521.
4. Cheng, S.-Y.; Dai, C.-F.; Duh, C.-Y. *J. Nat. Prod.* **2007**, *70*, 1449–1453.
5. El-Gamal, A. A. H.; Wang, S.-K.; Dai, C.-F.; Duh, C.-Y. *J. Nat. Prod.* **2004**, *67*, 1455–1458.
6. Duh, C.-Y.; Wang, S.-K.; Chu, M.-J.; Sheu, J.-H. *J. Nat. Prod.* **1998**, *61*, 1022–1024.
7. Cheng, S.-Y.; Dai, C.-F.; Duh, C.-Y. *Steroids* **2007**, *72*, 653–659.
8. Shao, Z.-Y.; Zhu, D.-Y.; Guo, Y.-W. *J. Nat. Prod.* **2002**, *65*, 1675–1677.
9. Huang, Y.-C.; Wen, Z.-H.; Wang, S.-K.; Hsu, C.-H.; Duh, C.-Y. *Steroids* **2008**, *73*, 1181–1186.
10. (a) Ma, K.; Li, W.; Fu, H.; Koike, K.; Lin, W.; van Ofwegen, L.; Fu, H. *Steroids* **2007**, *72*, 901–907; (b) Rao, M. R.; Venkateshan, U.; Venkateswarlu, Y. *J. Nat. Prod.* **1999**, *62*, 1584–1585.

11. (a) Feller, M.; Rudi, A.; Berer, N.; Goldberg, I.; Stein, Z.; Benayahu, Y.; Kashman, Y. *J. Nat. Prod.* **2004**, *67*, 1303–1308; (b) Melching, St.; Bülow, N.; Wihstutz, K.; Jung, St.; König, W. A. *Phytochemistry* **1997**, *44*, 1291–1296.
12. *Erectathiol* (**1**): Primrose yellow oil; $[\alpha]_D^{24}$ +23 (*c* 0.4, $CHCl_3$); IR (KBr) υ_{max} 3035, 2927, 2864, 1633, 1456, 1372 cm^{-1}; ^1H NMR and ^{13}C NMR data, see Table 1; FABMS *m/z* 235 ($[M+H]^+$, 0.7); HRFABMS *m/z* 235.1521 $[M+H]^+$ (calcd for $C_{15}H_{23}S$, 235.1520).
13. Leriverend, C.; Metzner, P.; Capperucci, A.; Degl'Innocenti, A. *Tetrahedron* **1997**, *53*, 1323–1342.
14. *(2E,6E)-3-Isopropyl-6-methyl-10-oxoundeca-2,6-dienal* (**3**): Primrose yellow oil; UV (MeOH) λ_{max} (log ε) 241 (3.81) nm; IR (KBr) υ_{max} 2963, 2932, 2874, 1716, 1671, 1625, 1463, 1363, 1155 cm^{-1}; ^1H NMR and ^{13}C NMR data, see Table 1; ESIMS *m/z* 259 $[M+Na]^+$; HRESIMS *m/z* 259.1676 $[M+Na]^+$ (calcd for $C_{15}H_{24}O_2Na$, 259.1674).
15. *Chabrosterol* (**4**): White amorphous powder; $[\alpha]_D^{25}$ +28.5 (*c* 0.1, $CHCl_3$); IR (KBr) υ_{max} 3309, 2933, 2868, 1723, 1685, 1462, 1376, 1209 cm^{-1}; ^1H NMR and ^{13}C NMR data, see Table 2; ESIMS *m/z* 421 $[M+Na]^+$; HRESIMS *m/z* 421.3085 $[M+Na]^+$ (calcd for $C_{27}H_{42}O_2Na$, 421.3082).
16. Bortolotto, M.; Braekman, J. C.; Daloze, D.; Losman, D.; Tursch, B. *Steroids* **1976**, *28*, 461–466.
17. Cheng, S.-Y.; Wen, Z.-H.; Chiou, S.-F.; Wang, S.-K.; Hsu, C.-H.; Dai, C.-F.; Chiang, M. Y.; Duh, C.-Y. *Tetrahedron* **2008**, *64*, 9698–9704.